The Spitzer Space Telescope: New Views of the Cosmos
ASP Conference Series, Vol. 357, 2006
L. Armus and W.T. Reach

Large Scale Structure at 24 Microns in the SWIRE Survey

Frank J. Masci and the SWIRE Team

Spitzer Science Center, California Institute of Technology, 220-6, Pasadena, CA, 91125

Abstract. We present initial results of galaxy clustering at 24μm by analyzing statistics of the projected galaxy distribution from *counts-in-cells.* This study focuses on the ELAIS-North1 SWIRE field. The sample covers $\simeq 5.9\,\mathrm{deg}^2$ and contains 24,715 sources detected at 24μm to a 5.6σ limit of 250μJy (in the lowest coverage regions). We have explored clustering as a function of 3.6 - 24μm color and 24μm flux density using angular-averaged two-point correlation functions derived from the variance of counts-in-cells on scales $0^{\circ}.05 - 0^{\circ}.7$. Using a power-law parameterization, $w_2(\theta) = A(\theta/\mathrm{deg})^{1-\gamma}$, we find $[A, \gamma] = [(5.43 \pm 0.20) \times 10^{-4}, 2.01 \pm 0.02]$ for the full sample (1σ errors throughout). We have inverted Limber's equation and estimated a spatial correlation length of $r_0 = 3.32 \pm 0.19\,h^{-1}$Mpc for the full sample, assuming stable clustering and a redshift model consistent with observed 24μm counts. We also find that blue $[f_\nu(24)/f_\nu(3.6) \leq 5.5]$ and red $[f_\nu(24)/f_\nu(3.6) \geq 6.5]$ galaxies have the lowest and highest r_0 values respectively, implying that redder galaxies are more clustered (by a factor of ≈ 3 on scales $\gtrsim 0^{\circ}.2$). Overall, the clustering estimates are smaller than those derived from optical surveys, but in agreement with results from IRAS and ISO in the mid-infrared. This extends the notion to higher redshifts that infrared selected surveys show weaker clustering than optical surveys.

Analysis and Summary

The *Spitzer* Wide-area Infrared Extragalactic legacy program (SWIRE; Lonsdale et al. 2003) is expected to detect over two million galaxies at infrared wavelengths from 3.6 to 160μm over $49\,\mathrm{deg}^2$ and to redshifts $z \simeq 2.0$. Our ELAIS-N1 sample corresponds to a completeness of $\simeq 90\%$ and we used a $\simeq 5.9\,\mathrm{deg}^2$ central region where the completeness was uniform to within $\pm 0.5\%$. Reliability of each 24μm detection was ensured by requiring an IRAC 3.6μm association with SNR $\geq 10\sigma$ (where $0.6 \leq \sigma/\mu\mathrm{Jy} \leq 1.0$) and separation $\leq 2''$. Stars were identified and rejected using a combination of the 3.6μm stellarity index (≥ 0.9) and cuts in $f_\nu(3.6)$ versus $f_\nu(24)/f_\nu(3.6)$ flux ratio (see Masci et al. 2005). This study is the first of its kind at this wavelength and sensitivity, reaching a factor of ≈ 1000 deeper in flux density than the IRAS 25μm galaxy surveys.

The method of counts-in-cells (CICs; see Masci et al. 2005, and references therein) provides the full galaxy count distribution function within a cell of given size, and its moments are related to the classical n-point correlations. The variance in particular is related to the cell-averaged *two-point* correlation function. The advantage of CICs over traditional, direct binning methods is that the data does not require binning, moments from CICs have better signal-to-noise ratio properties, no random comparison sample is needed, and systematics from catalog boundaries and finite sampling are better handled.

Figure 1 (left panel) shows the angular-averaged correlation function as a function of cell diameter. The angular range corresponds to *comoving* scales of $\simeq 2 - 24\,h^{-1}$Mpc at the expected median redshift of $\simeq 0.8$ for the full sample, as predicted from the Xu et al. (2001) model and $(\Omega_m, \Omega_\Lambda) = (0.3, 0.7)$. The

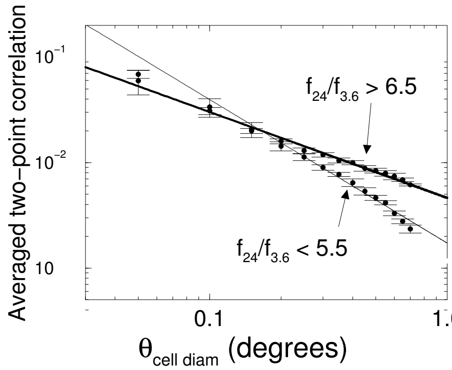

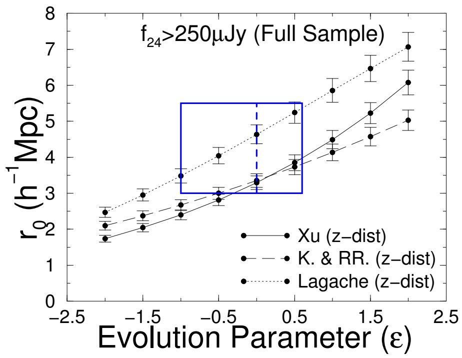

Figure 1. Angular-averaged correlation versus angular scale for two color subsamples (left) and correlation length versus the evolution parameter ϵ (right), assuming three different model redshift distributions. The rectangle encloses a region consistent with predictions from N-body simulations and other observations.

striking feature is that redder (mid-IR excess) galaxies exhibit a stronger projected clustering than blue galaxies on scales $\gtrsim 0^\circ.2$. This difference is difficult to explain by varying projection effects since their *photometric* redshift distributions (although incomplete) are not too dissimilar. More work is needed to verify this.

We have estimated correlation lengths by inverting Limber's equation with three different model redshift distributions and assuming a simple evolution model for 3D clustering: $\xi(r,z) = (r/r_0)^{-\gamma}(1+z)^{-(3+\epsilon)}$, where r is a proper coordinate and $\epsilon = 0$ implies constant (stable) clustering in proper coordinates. We found spatial correlation lengths in the range $r_0 \simeq 3.3$ to $4.7\,h^{-1}$Mpc for the full sample assuming $\epsilon = 0$ (right panel in Fig. 1). For the redshift model of Xu et al. (2001), whose predictions agree remarkably well with observed 24μm counts (e.g., Chary et al. 2004), we find $r_0 = 3.32 \pm 0.19\,h^{-1}$Mpc. We also found that red galaxies are more clustered by a factor of ~ 2.6 in their spatial correlation amplitude on $5\,h^{-1}$Mpc scales at $z = 0$ than blue galaxies (not shown). This may suggest that merger driven starbursts are dominating the mid-infrared excess population at $z \gtrsim 0.5$. We note however that our 3D clustering estimates depend strongly on the assumed redshift distribution. This reinforces the need to establish the redshift distribution of SWIRE galaxies.

Acknowledgments. Support for this work was provided by NASA through an award issued by the Jet Propulsion Laboratory, California Institute of Technology under NASA contract 1407.

References

Chary, R. et al. 2004, ApJS, 154, 80
King, A. J., and Rowan-Robinson, M. 2003, MNRAS, 339, 260
Lagache, G. et al. 2003, MNRAS, 338, 555
Lonsdale, C. J. et al. 2003, PASP, 115, 897
Masci, F. J. et al. 2005, ApJ, (in preparation)
Xu, C. K. et al. 2001, ApJ, 562, 179